Evolution of temperature, O_3, CO, and N_2O profiles during the exceptional 2009 Arctic major stratospheric warming as observed by lidar and mm-wave spectroscopy at Thule (76.5°N, 68.8°W), Greenland.

Claudia Di Biagio[1,2], Giovanni Muscari[3], Alcide di Sarra[1], Robert L. de Zafra[4], Paul Eriksen[5], Giorgio Fiocco[6], Irene Fiorucci[3], and Daniele Fuà[6]

[1] ENEA/UTMEA-TER, S. Maria di Galeria, Italy
[2] Department of Earth Science, University of Siena, Siena, Italy
[3] Istituto Nazionale di Geofisica e Vulcanologia, Rome, Italy
[4] Department of Physics and Astronomy, Stony Brook University, Stony Brook, NY, USA
[5] Danish Meteorological Institute, Copenhagen, Denmark
[6] Department of Physics, "Sapienza" University of Rome, Rome, Italy

Authors

Claudia Di Biagio
ENEA/UTMEA-TER, via Anguillarese 301, 00123, S. Maria di Galeria (Rome), Italy
Phone: 0039 06 30486127
claudia.dibiagio@enea.it

Giovanni Muscari
Istituto Nazionale di Geofisica e Vulcanologia, Via di Vigna Murata 605, 00143, Rome, Italy
Phone: 0039 06 51860724
giovanni.muscari@ingv.it

Alcide di Sarra
ENEA/UTMEA-TER, via Anguillarese 301, 00123, S. Maria di Galeria (Rome), Italy
Phone: 0039 06 30484986
alcide.disarra@enea.it

Robert L. de Zafra
Department of Physics and Astronomy, Stony Brook University, New York, USA
Phone: 001 631 6328137
rdezafra@notes.cc.sunysb.edu

Paul Eriksen
Danish Meteorological Institute, Danish Climate Centre
Lyngbyvej 100, DK-2100, Copenhagen, Denmark
Phone : 0045 39157418
pe@dmi.dk

Giorgio Fiocco
Department of Physics, "Sapienza" University of Rome, Piazzale Aldo Moro 2, 00185, Rome, Italy
Phone: 0039 06 49913513
giorgio.fiocco@uniroma1.it

Irene Fiorucci
Istituto Nazionale di Geofisica e Vulcanologia, Via di Vigna Murata 605, 00143, Rome, Italy
Phone: 0039 06 51860719

irene.fiorucci@ingv.it

Daniele Fuà

Department of Physics, “Sapienza” University of Rome, Piazzale Aldo Moro 2, 00185, Rome, Italy

Phone: 0039 06 49913515

daniele.fua@uniroma1.it

Abstract

The 2009 Arctic sudden stratospheric warming (SSW) was the most intense event of this kind ever observed. Unique ground-based measurements of middle atmospheric profiles for temperature, O_3, CO, and N_2O obtained at Thule (76.5°N, 68.8°W), Greenland, in the period January – early March are used to show the evolution of the 2009 SSW in the region of its maximum intensity. The first sign of the SSW was detected at θ~2000 K on January 19, when a rapid decrease in CO mixing ratio took place. The first evidence of a temperature increase was observed at the same level on 22 January, the earliest date on which lidar measurements reached above ~50 km. The warming propagated from the upper to the lower stratosphere in 7 days and the record maximum temperature of 289 K was observed between 1300 and 1500 K potential temperature on 22 January. A strong vortex splitting was associated with the SSW. Stratospheric backward trajectories indicate that airmasses arriving to Thule during the warming peak underwent a rapid compression and an intense adiabatic warming of up to 50 K. The rapid advection of air from the extra-tropics was also occasionally observed to produce elevated values of N_2O mixing ratio. Starting from mid-February the temperature profile and the N_2O mixing ratio returned to the pre-warming values in the mid and upper stratosphere, indicating the reformation of the vortex at these levels. In late winter, vertical descent from starting altitudes of ~60 km is estimated from CO profiles to be 0.25±0.05 km/day.

INDEX TERMS: 0340 (middle atmosphere: composition and chemistry), 0341 (middle atmosphere: constituent transport and chemistry), 3334 (middle atmosphere dynamics), 3360 (remote sensing)

KEYWORDS: sudden stratospheric warming, winter polar stratosphere, temperature, O_3, N_2O, CO.

1. Introduction

Sudden Stratospheric Warmings are the most important perturbing events that affect the dynamics and thermal structure of the winter stratosphere in the Northern Hemisphere. The 2008/09 Arctic winter has been characterized by the largest major SSW event ever observed [*Labtizke and Kunze,* 2009; *Manney et al*., 2009; *Harada et al.*, 2010]. The development of SSWs is linked to the vertical propagation of planetary waves, which dissipate first in the mesosphere and then progressively through the stratosphere, interacting with the westerly winter circulation and modifying the atmospheric thermal profile from the upper troposphere through the mesosphere [*Schoeberl et al*., 1978]. Major warmings produce the breakdown of the winter circulation through either the displacement or splitting of the polar vortex, the instauration of an easterly circulation, and the reversal of the latitudinal temperature gradient. Strong differences in terms of dynamics, transport, evolution of the stratospheric chemical composition and of the vertical structure of the polar vortex exist between displacement and splitting events [*Charlton and Polvani*, 2007; *Manney et al.*, 2009; *Matthewman et al.*, 2009]. Minor events are less intense and do not produce the reversal of the mean zonal circulation.

The Arctic stratosphere is characterized by large interannual variability and very warm winters can alternate with cold ones. The occurrence of SSWs has been shown to be connected to the phase of the Quasi Biennial Oscillation, to the solar cycle [*Labitzke and van Loon*, 1988], and to the Southern Oscillation [*van Loon and Labitzke*, 1987]. As discussed by *Charlton and Polvani* [2007], a frequent occurrence of sudden warmings occurred in the period 1958-2002, and a mean of six major events per decade was observed. Series of minor warmings or single minor events typically alternate with major SSWs [*Schoeberl*, 1978; *Manney et al*., 2005].

An increasing number of large warming events has been registered during the last ten years [*Manney et al*., 2005]. Before the winter of 2008/09, the most intense recent warmings in the Arctic were detected in 2004 and 2006 [*Manney et al*., 2005 and 2008].

The 2009 SSW to be described here using ground-based observations started in mid-January and was accompanied by an intensification of planetary wave number 2. As the SSW developed, the stratopause lowered and the mean zonal circulation reversed, proceeding from the mesosphere downwards. Studies by *Manney et al*. [2009] (using satellite-based measurements), by *Labitzke and Kunze* [2009] (using the European Centre for Medium-range Weather Forecast reanalyses), and by *Harada et al*. [2010] (using the Japan Meteorological Agency reanalyses) describe the mean evolution of the warming event over the entire Arctic region, thus providing a global view on the 2009 winter. The reversal of the 10 hPa zonal mean zonal wind at 60°N occurred at around 22 January [*Manney et al.*, 2009]. As the SSW propagated downward, it induced a splitting of the polar vortex in the lower stratosphere. The maximum warming at 10 hPa took place on 24 January above Greenland due to the dominant planetary wave 2 [*Labitzke and Kunze*, 2009] during the SSW. At the end of January the stratopause disappeared and a quasi-isothermal stratospheric temperature profile was observed. A strong polar vortex reformed very rapidly in the upper stratosphere at the beginning of February. The 10 hPa 60°N westerly circulation was restored at the beginning of March.

In the present study, ground-based observations of the thermal structure and chemical composition of the middle atmosphere from the Network for Detection of Atmospheric Composition Change (NDACC, *http://www.ndsc.ncep.noaa.gov/*) station at Thule Air Base (76.5°N, 68.8°W), Greenland, are used to show the evolution of the phenomenon and its interactions with the dynamical structure of the polar vortex in the region of maximum warming [*Labitze and Kunze*, 2009].

2. Measurements

An intensive measurement campaign was conducted at Thule during January–early March, 2009, with a lidar ("Sapienza" University of Rome) and a ground-based millimeter-wave spectrometer (Stony Brook University). The lidar was installed at Thule in 1990 and has been operational during several years, particularly during the winter season [i.e., *di Sarra et al.*, 2002 and references therein; *Keckhut et al.*, 2004]. The transmitter of the lidar system is composed of a two stage Nd:YAG laser with second harmonic generator producing linearly polarized pulses of a nominal energy of ~200 mJ at 532 nm, with a repetition rate of 10 Hz. The divergence of the laser beam is less than 1 mrad. The receiver includes a 0.8 m diameter Cassegrain telescope and a photon counting acquisition system. The parallel and cross polarized components of the backscattered signal are separately acquired. A chopper is used to cut off signals from the lowest atmospheric levels in order to prevent the saturation of the photomultiplier tubes. Atmospheric temperature (T) profiles were derived from 25 km up to 70 km altitude by applying the algorithm described by *Marenco et al.* [1997]. T was derived with a vertical resolution of 150 m and averaged over 4.5 km. To reduce the signal-to-noise ratio, the signal was integrated for 1-5 hours, depending on the weather conditions. The estimated 1σ uncertainty varies from ~1 K at 25 km to ~15 K at the maximum probed altitude. National Centers for Environmental Predictions (NCEP) reanalyses over Thule and radiosonde data obtained from the stations of Eureka (79.9°N, 85.9°W) and Alert (82.5°N, 62.3°W) were used to provide temperatures below 25 km.

The ground-based millimeter-wave spectrometer (GBMS) has been operated most recently prior to 2009 at Thule during the winters of 2001-2002 and 2002-2003 [*Muscari et al.*, 2007, and references therein]. The GBMS measures rotational emission spectra of atmospheric chemical species such as O_3, N_2O, CO and HNO_3, as well as the H_2O continuum, with a spectral window of 600 MHz tunable between approximately 230 and 280 GHz. It comprises a front end receiver employing a cryogenically cooled SIS mixer and a back end composed of an Acousto-Optical Spectrometer (AOS) [*de Zafra*, 1995]. By means of the observed line shape together with pressure and temperature vertical profiles, a mathematical deconvolution process allows finding the emitting molecule's concentration as a function of altitude from about 15 to 80 km altitude. For water vapor, only the integrated column contents can be obtained [*Fiorucci et al.*, 2008]. O_3 and CO spectra are measured with a ~1.5-hour integration, while HNO_3 and N_2O lines are weaker and need about 3-4 hours of integration. The vertical resolution of the GBMS is limited by the inversion algorithm and averages one pressure scale height: the nominal vertical resolution is 6-8 km, although relative peaks in concentration profiles can be determined within ±1 km altitude. Detailed information on the observing technique, and GBMS data analysis can be found in *de Zafra* [1995], and *Muscari et al.* [2007].

GBMS retrieval algorithm has recently changed to a standard Optimal Estimation Method (OEM) which was applied to the O_3 and N_2O measurements reported here. Careful comparisons of mixing ratio (mr) profiles obtained with previous (*Muscari et al.* [2007], and references therein) and current algorithms show no significant differences in results and error estimates, with the OEM providing however additional information needed to better characterize the retrievals and compare them to other datasets. Further refinements and validation efforts on O_3 and N_2O OEM retrievals are still underway and results shown here should be considered preliminary. CO retrievals, instead, have not yet undergone such testing and vertical profiles reported in this manuscript are therefore still obtained using the Chahine-Twomey method [*de Zafra and Muscari*, 2004, and references therein]. O_3, N_2O, and CO measurements have an estimated 1σ uncertainty of 13% (minimum 0.3 ppmv), 15% (minimum 5 ppbv), and 16% (minimum 0.1 ppmv), respectively.

During January- early March 2009, lidar and GBMS measurements were usually performed on a daily basis, except during periods characterized by poor weather conditions (both instruments, 5-11 February) or instrument malfunctioning (lidar, 16-22 January).

3. Results and discussion

3.1. Temporal evolution of the middle atmosphere thermal structure

Figure 1 shows the temporal evolution of temperature profiles measured by lidar between 14 January and 5 March 2009 at Thule. The maximum altitude in the derived temperature depends on the time of integration, presence of clouds, and background noise. Initial profiles reached only up to 45-50 km. The agreement between lidar temperature profiles and radiosonde data is generally good (see overlapped profiles in Figure 1), despite a distance of more than 400 km between Thule and both Eureka and Alert.

In mid-January, before the SSW event, a cold vortex was stably present (see Figure 1, profiles of 14 and 15 January, and Figure 7, maps of 17 January). An ozonesonde launched from Thule on 12 January showed that conditions for polar stratospheric cloud (PSC) formation were already present at that date at an altitude of about 19 km. Type Ia PSC particles were detected by lidar on January 17 and 18 between 17 and 22 km (not shown).

Starting from the 22 January, a sudden increase in the temperature profiles was observed in the region below about 50 km. Because initial lidar profiles reached only up to ~50 km, and because the lack of measurements between the 15 and the 22 January, the first thermal measure of warming was observed on 22 January, although we show below that a dramatic change in high altitude CO was seen to begin on 19 January.

Temperatures larger than 280 K were measured on January 22 between about 31 and 43 km altitude. On January 24 at the altitude of 30 km (~10 hPa) the temperature was 273 K, consistent with the warming peak values reported over Thule by *Labitzke and Kunze* [2009] in their Figure 4. The temperature profile became nearly isothermal over the wide vertical range 24-55 km at the end of January (days 27-28, T~240K), and then between approximately 15-45 km altitude at the beginning of February (days 35-37, T~230 K). From mid-February (days 43-44) to the beginning of March, the temperature profile returned to the pre-warming values above 35 km altitude, due to the restoration of the polar vortex (see

Figure 5), while remaining up to 30 K warmer than in the pre-warming period at lower levels, where the vortex never reformed during the time monitored here.

On January 22 the stratopause (identified as the height of maximum stratospheric temperature) was observed at about 35 km altitude. It descended to about 30 km on 25 January. With the development of the isothermal profile noted in the preceeding paragraph, a local maximum appeared at about 25 km on the 26th, progressively descending to 20 km on 29 January. In early February a T maximum appeared near 52 km, and remained between 45 and 55 km until early March.

Figure 2 shows the temporal evolution of T at different potential temperature (θ) levels between 400 and 2000 K (approximately 16 to 50 km) during the period 14 January – 5 March 2009 (days 14-64). The highest temperatures occurred on 22 January at the highest sounded levels. The warming reached 800-1000 K after 2-4 days (January 24-26), and 400-600 K after 6-7 days (January 28-29). The value of the maximum T reached at each level due to the downward propagation of the warming decreased approximately linearly with θ from 289 K at layers between 1300 and 1500 K (22 January) to 222 K at level 400 K (30 January).

In order to relate the warming event to the dynamical situation, we calculated temperature variations along 5-day isentropic backward airmass trajectories arriving at Thule. Trajectories were obtained from the NASA-GSFC Automailer system [*Schoeberl and Sparling*, 1994] using NCEP reanalysis data. One trajectory per day ending at Thule at 00 UT was used in the analysis. The difference ΔT between the airmass final temperature over Thule and the minimum T reached by the air parcel during its 5-day run is indicative of the adiabatic heating taking place along the trajectory. Figure 3 shows the temporal evolution of ΔT for θ levels between 400 and 2000 K in the period 1 January – 5 March (days 1-64). ΔT is always <10 K at all levels, except when the warming occurs. ΔT for the days of maximum warming is ~50 K at 1000÷1300 K and between 25 and 45 K at the other selected θ levels. The corresponding airmass compression Δp, measured as the difference between the air parcel final pressure over Thule and the minimum pressure reached along its 5-days isentropic trajectory, is estimated to produce a 30-50% pressure increment. The compression occurs later at the lowest levels, consistently with the evolution of the warming. Thus, air parcels on the trajectories approaching the polar region during the warming peak were subjected to a rapid compression and an intense adiabatic heating that largely contributed to the total observed warming.

3.2 Previous SSWs measured at Thule by lidar

Figure 4 shows the temporal evolution of the temperatures measured by lidar at θ levels between 700 and 2000 K for the winters 2002, 2003, 2007, and 2009, all affected by major warmings. It should be pointed out that the two previously most intense SSWs of the decade were the ones of 2004 and 2006 [*Manney et al*., 2005 and 2008]; no lidar measurements were carried out at Thule during these two winters, so we can not directly relate the 2009 SSW with the warmings of 2004 and 2006. However, *Manney et al*. [2009] have already compared the three events and have shown that the 2009 warming was more intense than those of 2004 and 2006, producing stronger and more prolonged effects on the lower stratospheric dynamics and structure.

The 2009 SSW was characterized by the largest absolute temperatures and by the largest temperature gradient versus time ever observed at Thule by lidar. The maximum temperature of 289 K at 42-45 km (potential temperature levels between 1300 and 1500 K) is up to 40 K larger than maxima observed during winters 2002, 2003, and 2007 and the T gradient peaked at 42 km with ~9 K/day between 14 and 22 January. Temperatures between 35 and 45 km altitude (1000-1500 K potential temperature levels) were consistently lower throughout February and early March than in the other winters considered here.

3.3 Chemical composition and vortex evolution

Figure 5 shows the temporal evolution of Ertel's potential vorticity (PV), T, N_2O, CO, and O_3 mixing ratios above Thule, at different θ levels between 500 (~18-20 km) and 2000 K (~48-50 km), in the period 14 January – 5 March 2009. The PV values were obtained from the NASA-GSFC Automailer system, based on NCEP data. Estimates of PV values corresponding to the inner vortex edge during January are also given in Figure 5. Figure 6 shows polar plots obtained using Aura/MLS measurements from 13 January 2009, downloaded from *http://mls.jpl.nasa.gov/data/gallery.php* (courtesy of Gloria Manney). They are used here to show the overall chemical and dynamical status of the Arctic region before the SSW. Approximate values of N_2O and CO at the various potential temperature levels can be read on the corresponding scales and are consistent with GBMS values reported in Figure 5. Figure 6 shows that extravortex stratospheric air is richer in N_2O and poorer in CO with respect to in-vortex air. Upper stratospheric Aura/MLS maps for O_3 are useful to show that a combination of photochemistry and dynamics causes large O_3 gradients between the vortex edge and its inner region (characterized by little sun exposure and small O_3 mixing ratios).

PV values in Figure 5 show that the splitting of the vortex, concurrent with the passage of the vortex edge above Thule, progressed from the top downward and took about 8 days to reach the lower stratosphere (about 20 January at 2000 K, and 28 January at 500 K). Figure 7 shows Northern hemisphere PV maps (obtained from ECMWF reanalysis data) at the potential temperature levels of 950 and 550 K for selected days between 17 and 30 January. At 950 K the vortex was stably present above Thule until the 22-23 January, when the splitting occurred at this level and the transition from inside to outside the vortex caused the rapid decrease in PV. This transition was not observed at Thule until 27 January at 550 K. These results are in agreement with our analyses at 1000 K and 500-600 K, respectively, based on PV data shown in Figure 5.

As apparent in Figure 5, between 1000 and 500 K the passage of the vortex edge over Thule associated with the vortex breakup, was accompanied by a sudden increase in N_2O mr which occurred between January 26 and 28. The observed increase brought N_2O mr values of about 0.25, 0.15, 0.10, and 0.08 ppmv at 500, 600, 800 K, and 1000 K, respectively, values representative of low- to mid-latitude air (see also Figure 6). At all these levels, PV and N_2O are in good agreement in identifying the vortex breakup (decreasing PV, increasing N_2O), although the exact timing might be slightly off depending on the PV value chosen as indicative of the vortex inner edge. Figure 8 shows isentropic 10-days backward airmass trajectories obtained from the NASA-GSFC Automailer system for the levels 500, 800, and 1500 K ending at Thule at 00:00 UT on 17, 23, and 30 January, 15 February, and 1 March 2009. At 500 K and 800 K, until the end of January, when the vortex breakup occurred, airmass trajectories indicate the presence of a typical vortex circulation (trajectories for 17 and 23 January); from the end of January, airmasses from mid- and low-latitudes were advected over Thule (see for example the trajectory for 30 January at 800 K), thus explaining the rapid increase in N_2O mr immediately after the vortex breakup.

At higher levels, because of the rapid vertical decrease in both nitrous oxide mr and its gradient across the vortex edge, N_2O becomes less reliable in describing the origin of the observed airmasses. Instead, CO becomes a better tool for this purpose [e.g., *de Zafra and Muscari*, 2004]. At these levels, the vortex splitting and the vortex edge transit over Thule was marked by a rapid decrease in CO mr matching the PV decrease. CO data in Figure 5 indicate that at 2000 K and 1500 K the vortex broke up over Thule on January 19-20. GBMS CO mr variations during the warming were observed to be about -0.2 and -0.35 ppmv/day at 1500 and 2000 K, respectively.

Concurrently, as warm, O_3-rich air from outside the vortex moved over Thule during the SSW, the GBMS measured an increase in O_3 mr in the upper stratosphere of 0.8 and 0.6 ppmv/day at 1500 and 2000 K, respectively. Airmasses coming from low- and midlatitudes were advected over Thule at 1500 K in the same period (see the trajectories for 23 and 30 January in Figure 8).

On late 25 January, shortly after the vortex breakup, a decrease in O_3 mr (about 3.6 ppmv) concurrent with a rapid and strong increase in CO mr (about 1.2 ppmv) between 1700 and 2000 K (only level 2000 K is shown in Figure 5) suggests that a parcel originating from the former inner vortex was advected over Thule at these levels (see also the O_3 and CO distribution in the inner vortex region from the AURA/MLS maps in Figure 6). This parcel of vortex air above Thule is not present in the PV reanalysis data. This indicates that GBMS tracer measurements may identify air parcels more accurately than PV reanalyses, which have an inherent coarser temporal and spatial resolution.

After such an intense SSW, air parcels in the newly formed vortex can be characterized by very different chemical tracer contents. The history of air masses contained in this re-formed vortex is therefore defined by their tracer concentrations (which are related to chemical and dynamics processes) more accurately than by their position inside the vortex (i.e., PV values, which are due to the radiative cooling in the polar night region) and a strict consistency between chemical tracer mr and PV values should not be expected. During February, PV values indicate that the vortex reformed rapidly and strongly at higher levels (between about 6 and 12 February at 2000, 1500, and 1000 K) but not in the lower stratosphere (below about 800 K). Figure 8 shows that a stable winter circulation, with airmasses confined inside the polar vortex, was restored at the 1500 K level starting from the second half of February.

At 500 K stable conditions with no vortex reformation were maintained until early March and the observed N_2O mr remained almost constant (about 0.3 ppmv) since the beginning of the SSW event, thus indicating well mixed extra-vortex airmasses. This is in agreement with backtrajectory analyses which indicate the advection of airmasses originating from mid- and high-latitudes over Thule (see Figure 8). At 800 K, the N_2O mr shows more variability with respect to level 500 K, with larger values from immediately after the warming event (day 27) through mid-February, indicating extra-vortex air masses, and smaller values from day 50 to the end of the campaign, indicating the observation of vortex air. Figure 8 shows airmasses from North Africa arriving over Thule on 30 January and on 15 February, therefore explaining the increase and the two relative maxima of N_2O mr at 800 K (~0.11 ppmv) observed on these two days. Additional Aura MLS contour maps at 850 K (*http://mls.jpl.nasa.gov/data/gallery.php*) show that complex structures of filaments of both residual and new vortex air formed during February and early March above the entire Arctic area, and the presence of these filaments may in part explain the observed N_2O and O_3 variability. At 1000 K, after the SSW event, the N_2O mr rapidly returns to low values, indicating the rapid reformation of a strong vortex with somewhat mixed vortex and mid-latitude air inside.

CO mr values at 1000 K and above 2000 K (data not shown) suggest the same scenario, with a rapid return to larger values shortly after the SSW and some variability due to vortex and extra vortex filaments (e.g., a sudden drop on day 42 at 1000 K matching in time the large O_3 mr peak shown in Figure 5). In an extended altitude range from 1300 K to 2000 K, however, CO does not show the same significant increase in mr from early February onward (see Figure 5) and the GBMS must be sampling extra-vortex air inside the re-formed vortex, as discussed previously. Figure 9 shows a contour plot of CO mr between 45 and 70 km in the period 14 January – 5 March (days 14-64). From mid-February to early March GBMS CO observations followed the vertical descent of air inside the reestablished polar vortex which results from the return flow of the meridional residual circulation. Seven different CO mr levels, from 5 to 11 ppmv, were followed as they descended with time inside the vortex and 3 of these linear regressions (for 5, 8 and 11 ppmv) are indicated in Figure 9 with black dashed lines. In mid-February, the indicated range of CO mr values encompasses descent starting altitudes between 58 and 62 km. The 7 linear regressions (all characterized by a squared correlation coefficient larger than 0.83) indicate descent rates from 0.20±0.05 to 0.30±0.05 km/day, gradually increasing with increasing starting altitude. We compared these estimates with approximate values that can be extrapolated from Figure 2 and 4 of Orsolini et al. Using their 4 and 5 ppmv Odin/SMR H_2O mr contour lines (located, at the beginning of February, approximately at 0.08 hPa or 62 km and 0.13 hPa or 59 km) we estimate a descent rate of 0.3 km/day (following the 4 ppmv contour) and 0.2 km/day (following the 5 ppmv contour). Although the agreement with our descent rates is very good, it should be underlined that the estimates obtained from the work of Orsolini et al. are based on data averaged over the whole polar region northward of 70°N.

4. Summary

Ground-based measurements of middle atmospheric profiles of temperature, O_3, CO, and N_2O mr were carried out from Thule, Greenland, during winter 2008-2009. These measurements add further information to previous analyses aimed at studying the evolution of the 2009 winter stratosphere and to tracking the exceptional SSW that occurred during the second half of January. Main findings of this analysis are:

1. In the first part of January the polar vortex was stable and cold. PSCs were detected between 17 and 22 km on 18-19 January (not shown).

2. At Thule, the SSW event was initially detected at θ~2000 K on January 19 by a rapid decrease in CO mr. The first evidence of a temperature increase was observed at about 50 km on 22 January, when lidar measurements were first able to reach this altitude. The warming progressed downward reaching about 15 km altitude on 29 January. The maximum physical temperature, 289 K, was observed at layers between 1300 and 1500 K on 22

January. In late January the temperature profile became near isothermal, particularly in the altitude layer between 15 and 45 km.

3. Backward trajectories at the various altitudes studied indicate that airmasses approaching the polar region during the warming peak were subjected to a rapid compression and an intense adiabatic warming. This is estimated to maximize with ΔT ~50 K at ~1000÷1300 K.

4. The passage of the vortex edge over Thule associated with the vortex breakup was marked by a sudden increase in N_2O and decrease in CO mixing ratios measured by the GBMS below and above 1000 K, respectively. PV, N_2O, and CO are in good agreement in identifying the vortex breakup. The vortex reformed rapidly and strongly above 1000 K at the beginning of February, but not in the lower stratosphere. Rapid changes in N_2O, O_3, and CO are associated with the advection of airmasses of different origins, in some cases not detected by PV analyses. Maxima in N_2O mr in late January and mid February are associated with rapid transport of extra-tropics airmasses.

5. Mesospheric CO measurements inside the reformed vortex indicate descent rates between (0.30 ± 0.05) and (0.20 ± 0.05) km/day for starting altitudes between 62 and 58 km, respectively, from mid-February to early March.

Acknowledgements

This work was supported by the project PRIN 2007 (“Dirigibile Italia”), funded by the Italian Ministry for University and Research, and by the Italian Antarctic Program. We would like to thank NSF and Susan Zager of CH2M HILL Polar Services for logistic support, and NASA-GSFC for the trajectory Automailer system. We are grateful to C.

Cesaroni for his assistance during the field campaign. Contributions by S. E. Ascanius, M. Cacciani, G. Casasanta, V. Ciardini, T. Di Iorio, and C. Tirelli are gratefully acknowledged. We thank Gloria Manney and the MLS team for making available the AURA/MLS data plots displayed in Figure 6. Helpful comments and suggestions from three anonymous reviewers are also acknowledged.

References

Barnett, J. J., and M. Corney (1985), Middle atmosphere reference model derived from satellite data, *Handbook for MAP*, *16*, 47-137.

Charlton, A.J., and L. Polvani (2007), A new look at stratospheric sudden warmings. Part I: climatology and modeling benchmarcks, *J. Climate*, 20, 449-469.

de Zafra, R. L. (1995), The ground-based measurements of stratospheric trace gases using quantitative millimeter wave emission spectroscopy, in *Diagnostic Tools in Atmospheric Physics, Proc. of the Int. Sch. of Phys. "Enrico Fermi",* vol. 124, 23– 54, Soc. It. di Fis., Bologna, Italy.

de Zafra, R. L., and G. Muscari (2004), CO as an important high-altitude tracer of dynamics in the polar stratosphere and mesosphere, *J. Geophys. Res.*, 109, D06105, doi:10.1029/2003JD004099.

di Sarra, A., M. Cacciani, G. Fiocco, D. Fuà, and T. S. Jørgensen (2002), Lidar observations of polar stratospheric clouds over northern Greenland in the period 1990-1997, *J. Geophys. Res.*, *107*(D12), doi:10.1029/2001JD001074.

Fiorucci, I., et al. (2008), Measurements of low amounts of precipitable water vapor by millimeter wave spectroscopy: An intercomparison with radiosonde, Raman lidar, and Fourier transform infrared data, *J. Geophys. Res.*, 113, D14314, doi:10.1029/2008JD009831.

Keckhut, P., et al. (2004), Review of ozone and temperature lidar validations performed within the framework of the Network for theDetection of Stratospheric Change, *J. Environ. Monit.*, *6*, 721–733.

Harada, Y., A. Goto, H. Hasegawa, and N. Fujikava (2010), A major stratospheric sudden warming event in January 2009, *J. Atmos. Sci.*, in press.

Labitzke, K, and H. Van Loon (1988), Associations between the 11-year solar cycle, the QBO and the atmosphere. Part I: The troposphere and the stratosphere in the Northern Hemisphere winter, *J. Atmos. Terr. Phys.*, *50*, 197-206.

Labitzke, K, and M. Kunze (2009), On the remarkable Arctic winter 2008/2009, *J. Geophys. Res.*, *114*, D00I02, doi:10.1029/2009JD012273.

Manney, G. L., et al. (2005), The remarkable 2003-2004 winter and other recent warm winters in Arctic stratosphere since 1990s, *J. Geophys. Res.*, *110*, D04107, doi:10.1029/2004JD005367.

Manney, G. L., et al. (2008), The evolution of the stratopause during the 2006 major warming: Satellite data and assimilated meteorological analyses, *J. Geophys. Res.*, *113*, D11115, doi:10.1029/2007JD009097.

Manney, G. L., et al. (2009), Aura Microwave Limb Sounder observations of dynamics and transport during the record-breaking 2009 Arctic stratospheric major warming, *Geophys. Res. Lett.*, *36*, L12815, doi:10.1029/2009GL038586.

Marenco, F., et al. (1997), Thermal structure of the winter middle atmosphere observed by lidar at Thule, Greenland, during 1993-1994, *J. Atmos. Sol-Terr. Phys*., *59* (2), 151-158.

Matthewman, N. J., J. G. Esler, A. J. Charlton-Perez, A. J., Polvani, L. M.(2009), A new look at stratospheric sudden warmings. Part III: Polar vortex evolution and vertical structure, *J. Clim.*, *22*, 1566-1585.

Muscari, G., et al. (2007), Middle atmospheric O_3, CO_2, N_2O, HNO_3, and temperature profiles during the Arctic winter 2001-2002, *J. Geophys. Res.*, *112*, D14304, doi:10.1029/2006JD007849.

Orsolini, Y. J., J. Urban, D. Murtagh, S. Lossow, and V. Lympasuvan (2010), Descent from the polar mesosphere and anomalously high stratopause observed in 8 years of water vapor and temperature satellite observations by the Odin Sub-Millimetre Radiometer, *J. Geophys. Res*., 115, D12305, doi:10.1029/2009JD013501.

Rodgers, C. D. (2000), Inverse Methods for Atmospheric Sounding: Theory and Practice, World Sci., Singapore.

Schoeberl, M.R., (1978), Stratospheric warmings: observations and theory, *Rev. Geophys. and Space Ge.*, *16* (4), 521-538.

Schoeberl M.R., and L. C. Sparling (1994), Trajectory Modelling; *Diagnostic Tools in Atmospheric Physics, Proc. S.I.F. Course CXVI*, edited by G. Fiocco and G. Visconti, North-Holland, Amsterdam, 1994.

Van Loon, H., and K. Labitzke (1987), The Southern Oscillation. Part V: the anomalies in the lower stratosphere of the Northern Hemisphere in winter and a comparison with the Quasi-Biennal Oscillation, *Mon. Weather Rev*., *115*, 357-369.

Figure captions

Figure 1. Lidar temperature profiles obtained between 14 January and 5 March 2009 at Thule. The T, T+σ, and T-σ are shown. The dashed line represents the CIRA 1986 model [*Barnett and Corney*, 1985] for the month. The dotted profiles are radiosonde data that are the closest in time data (from Eureka or Alert, depending on the data availability). The date, the time, and the integration time in minutes are reported.

Figure 2. Temporal evolution of stratospheric temperature interpolated at different θ levels between 400 and 2000 K (temperatures at 400, 500, and 600 K are from NCEP reanalyses) in the period 14 January – 5 March 2009 (days 14-64). The maximum 1σ uncertainty at the different levels is indicated by vertical bars. The maximum temperature obtained at each level due to the downward propagation of the warming is highlighted by a circle.

Figure 3. Temporal evolution of the temperature difference (ΔT) between the airmass final T over Thule and the minimum T reached by the air parcel along 5-day isentropic backward airmass trajectories for θ levels between 400 and 2000 K in the period 1 January – 5 March 2009 (days 1-64).

Figure 4. Temporal evolution of the temperature measured by lidar at various θ levels between 700 and 2000 K for the winters 2002, 2003, 2007, and 2009, all characterized by major warming events.

Figure 5. Temporal evolution of: a) Ertel's potential vorticity (1 PVU= 1 K m^2 kg^{-1} s^{-1}), N_2O and CO mr; b) O_3 mr and temperature, at θ levels between 500 and 2000 K in the period 14

January – 5 March 2009 (days 14-64). Temperatures at 500 and 600 K are from NCEP reanalyses. Horizontal dashed lines are indicative threshold values for the inner vortex edge.

Figure 6. Contour plots of Aura MLS O_3, N_2O and CO mixing ratios at three potential temperature levels on 13 January 2009 (courtesy of Gloria Manney and the MLS Team). White contours are typically scaled potential vorticity values from GEOS-5. For additional plots and information see *http://mls.jpl.nasa.gov/data/gallery.php*.

Figure 7. Northern hemisphere potential vorticity maps (obtained from ECMWF reanalysis data) at the potential temperature levels of 950 K (up) and 550 K (bottom) for 17-20-23-27-30 January 2009. Light grey lines corresponds to the inner vortex edge; black lines indicate the threshold temperatures for the formation of PSC at the two different levels. The position of Thule on the maps is indicated with a black point.

Figure 8. Isentropic 10-days backward airmass trajectories for the levels 500, 800, and 1500 K ending at Thule at 00:00 UT on 17-23-30 January, 15 February, and 1 March 2009. Trajectories were obtained from the NASA-GSFC Automailer system [*Schoeberl and Sparling*, 1994] using NCEP reanalysis data.

Figure 9. Contour plot of CO mr between 45 and 70 km in the period 14 January – 5 March 2009 (days 14-64). Linear fits to CO mixing ratio levels of 5, 8 and 11 ppmv altitude versus time are also shown (dashed lines).

Figure 1. Lidar temperature profiles obtained between 14 January and 5 March 2009 at Thule. The T, T+σ, and T-σ are shown. The dashed line represents the CIRA 1986 model [*Barnett and Corney*, 1985] for the month. The dotted profiles are radiosonde data that are the closest in time data (from Eureka or Alert, depending on the data availability). The date, the time, and the integration time in minutes are reported.

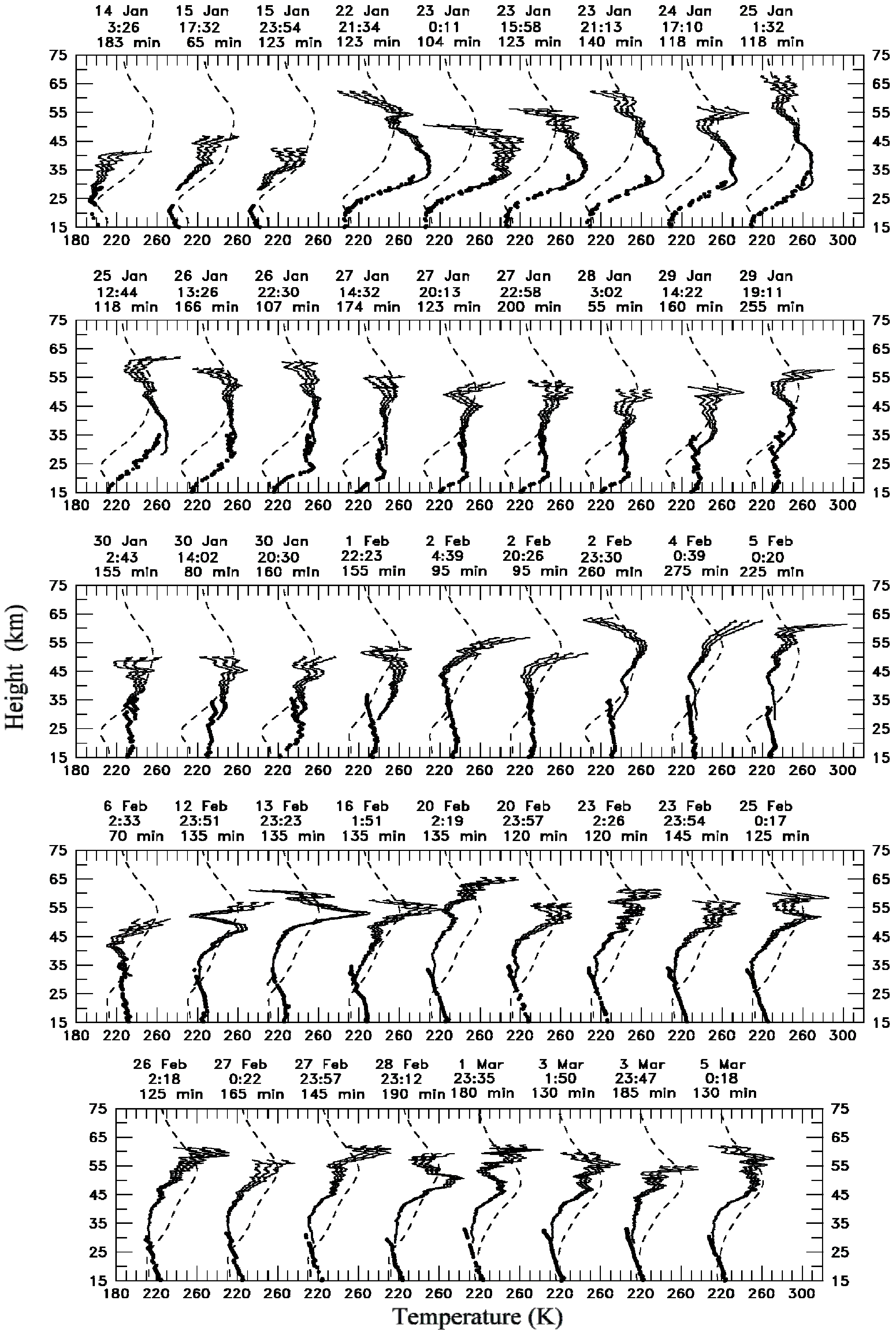

Figure 2. Temporal evolution of stratospheric temperature interpolated at different θ levels between 400 and 2000 K (temperatures at 400, 500, and 600 K are from NCEP reanalyses) in the period 14 January - 5 March 2009 (days 14-64). The maximum 1σ uncertainty at the different levels is indicated by vertical bars. The maximum temperature obtained at each level due to the downward propagation of the warming is highlighted by a circle.

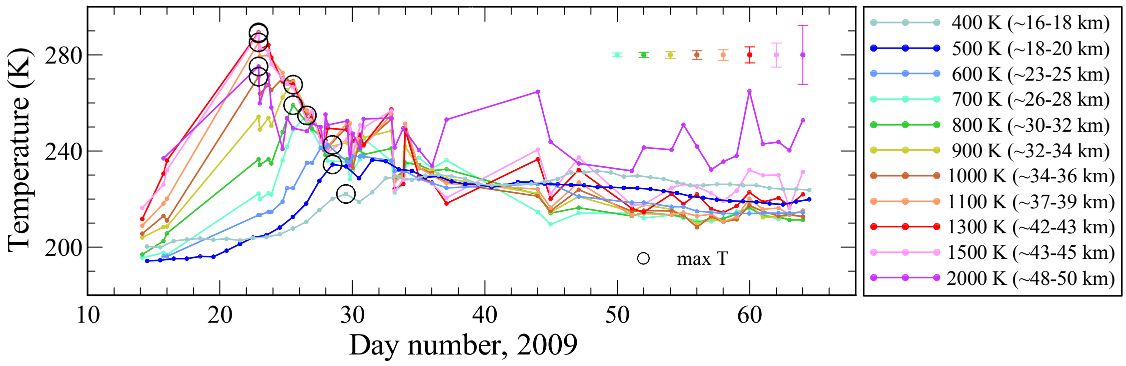

Figure 3. Temporal evolution of the temperature difference (ΔT) between the airmass final T over Thule and the minimum T reached by the air parcel along 5-day isentropic backward airmass trajectories for θ levels between 400 and 2000 K in the period 1 January- 5 March 2009 (days 1-64).

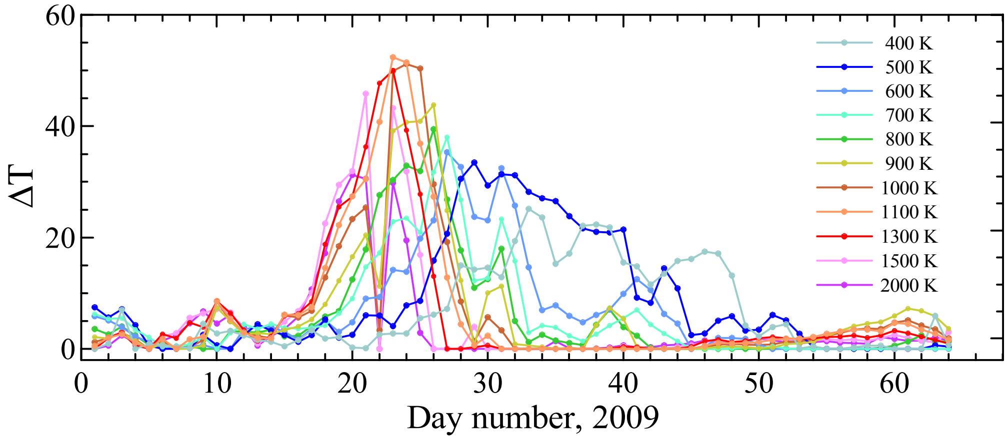

Figure 4. Temporal evolution of the temperature measured by lidar at various θ levels between 700 and 2000 K for the winters 2002, 2003, 2007, and 2009, all characterized by major warming events.

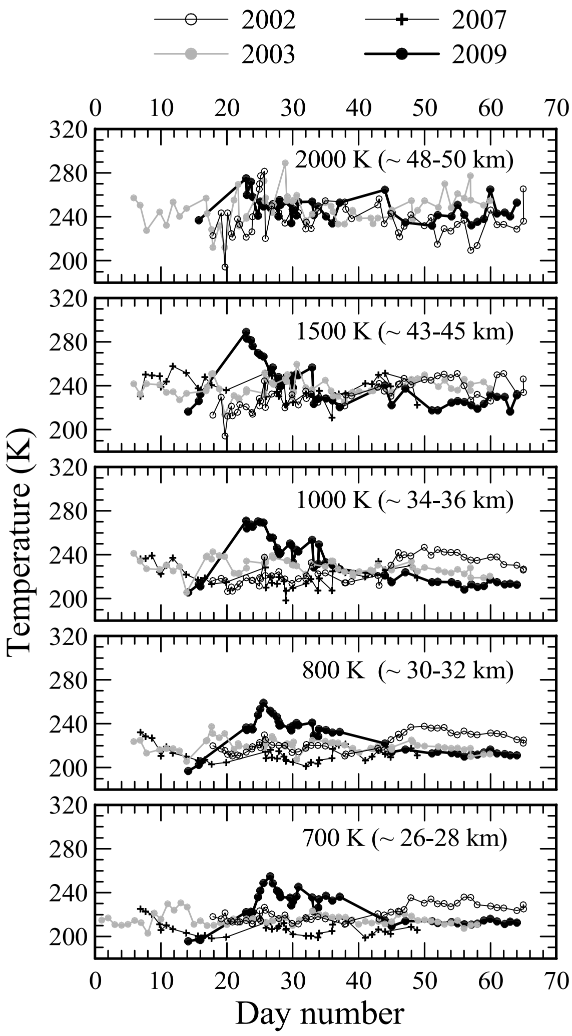

Figure 5. Temporal evolution of: a) Ertel's potential vorticity (1 PVU= 1 K m^2 kg^{-1} s^{-1}), N_2O and CO mr; b) O_3 mr and temperature, at θ levels between 500 and 2000 K in the period 14 January - 5 March 2009 (days 14-64). Temperatures at 500 and 600 K are from NCEP reanalyses. Horizontal dashed lines are indicative threshold values for the inner vortex edge.

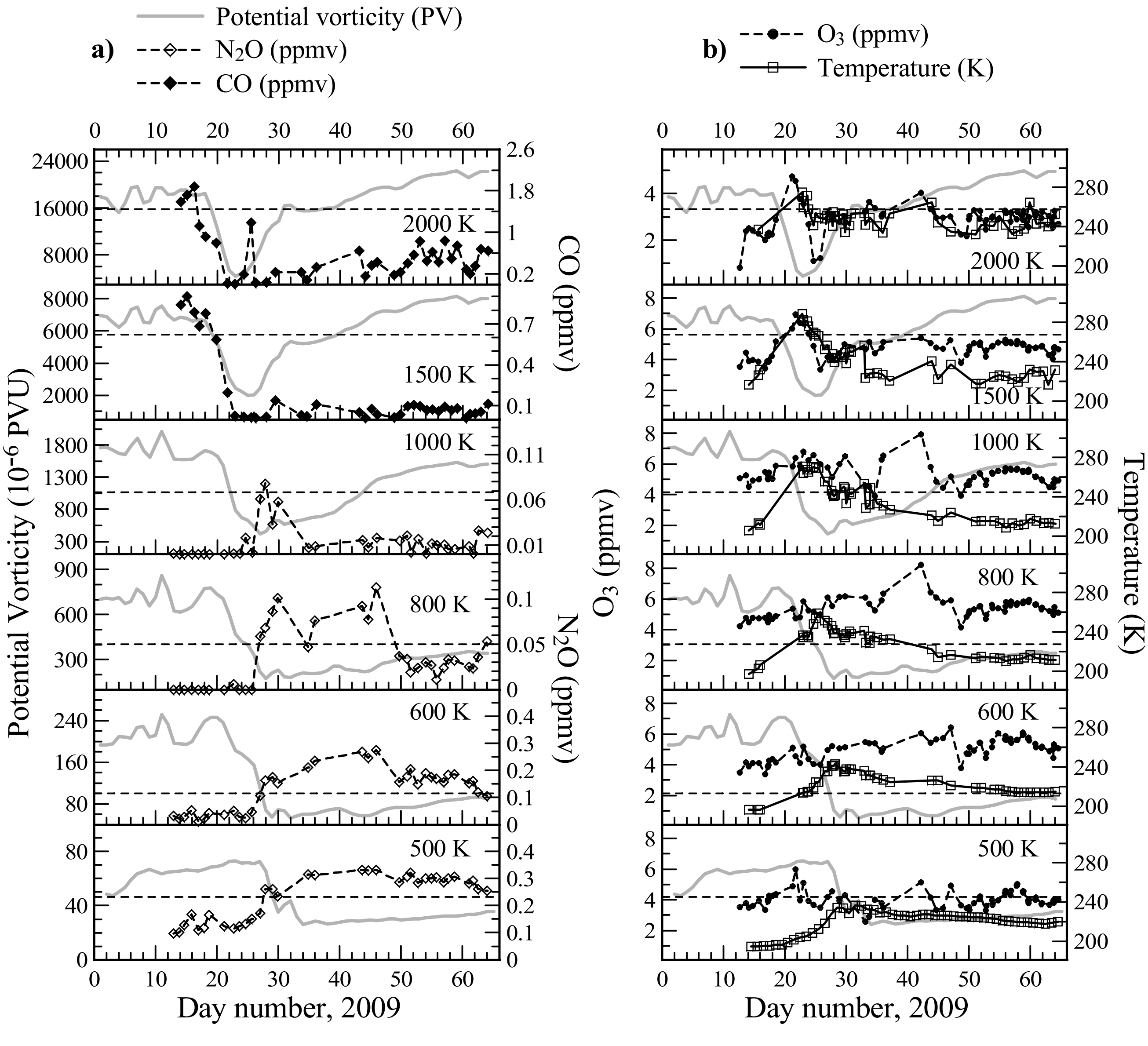

Figure 6: Contour plots of Aura MLS O3, N2O and CO mixing ratios at three potential temperature levels on 13 January 2009 (courtesy of Gloria Manney and the MLS Team). White contours are typically scaled potential vorticity values from GEOS-5. For additional plots and information see http://mls.jpl.nasa.gov/data/gallery.php.

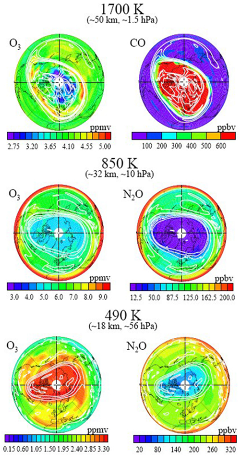

Figure 7. Northern hemisphere potential vorticity maps (obtained from ECMWF reanalysis data) at the potential temperature levels of 950 K (up) and 550 K (bottom) for 17-20-23-27-30 January 2009. Light grey lines corresponds to the inner vortex edge; black lines indicate the threshold temperatures for the formation of PSC at the two different levels. The position of Thule on the maps is indicated with a black point.

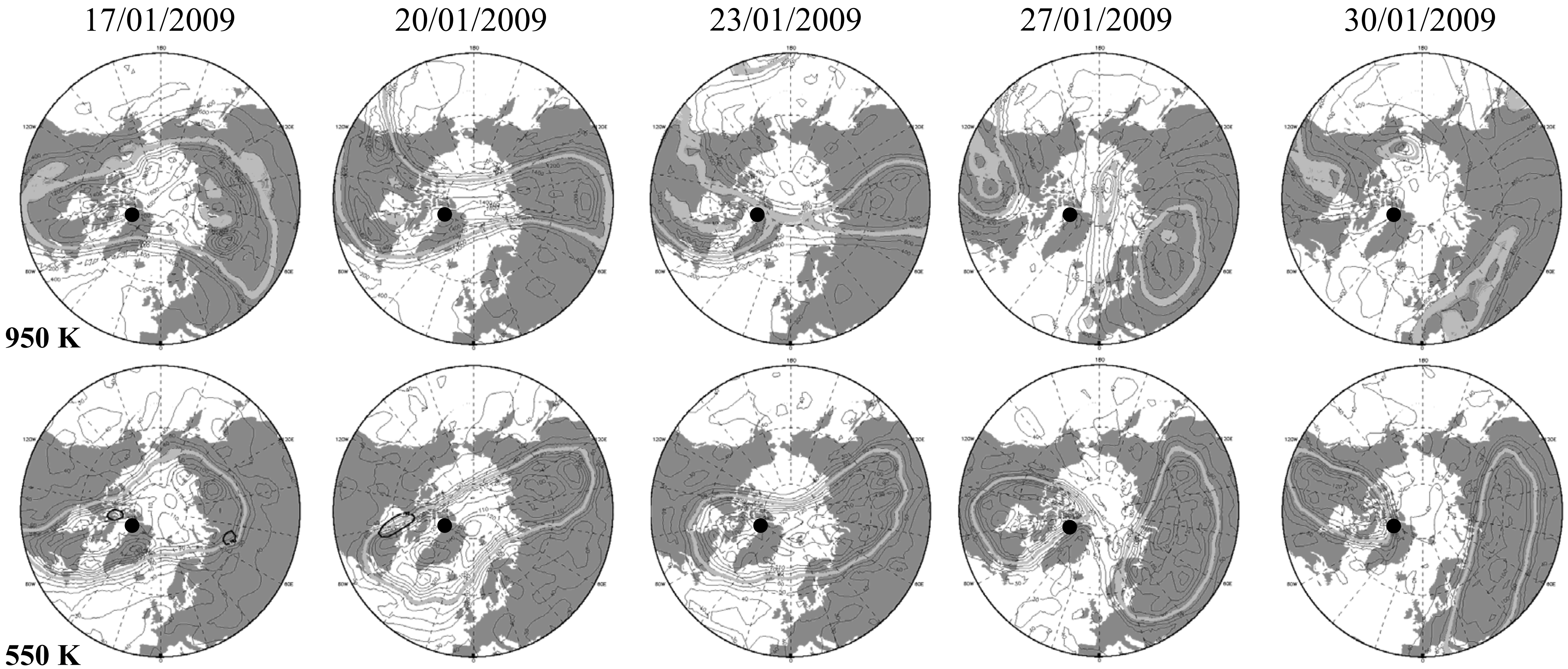

Figure 8. Isentropic 10-days backward airmass trajectories for the levels 500, 800 and 1500 K ending at Thule at 00:00 UT on 17-23-30 January, 15 February, and 1 March 2009. Trajectories were obtained from the NASA-GSFC Automailer system [*Schoeberl and Sparling*, 1994] using NCEP reanalysis data.

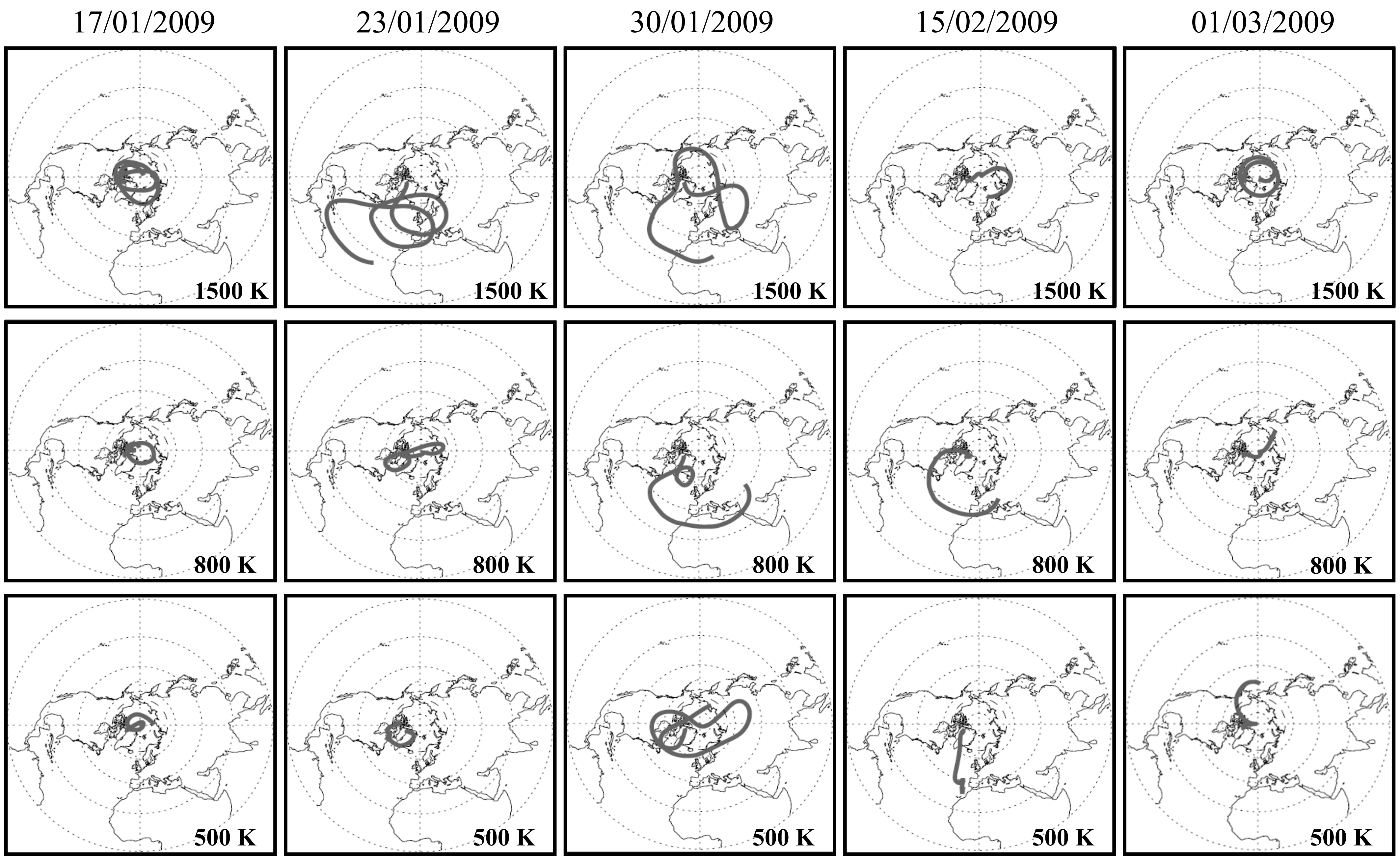

Figure 9. Contour plot of CO mr between 45 and 70 km in the period 14 January – 5 March 2009 (days 14-64). Linear fits to CO mixing ratio levels of 5, 8 and 11 ppmv altitude versus time are also shown (dashed lines).